Haemophilus ducreyi RpoE and CpxRA Appear To Play Distinct yet Complementary Roles in Regulation of Envelope-Related Functions

Dharanesh Gangaiah,[a] Xinjun Zhang,[d] Beth Baker,[f] Kate R. Fortney,[a] Yunlong Liu,[d] Robert S. Munson, Jr.,[f,g] Stanley M. Spinola[a,b,c,e]

Departments of Microbiology and Immunology,[a] Medicine,[b] Pathology and Laboratory Medicine,[c] and Medical and Molecular Genetics[d] and Center for Immunobiology,[e] Indiana University School of Medicine, Indianapolis, Indiana, USA; Center for Microbial Pathogenesis in the Research Institute at Nationwide Children's Hospital[f] and Department of Pediatrics,[g] The Ohio State University College of Medicine, Columbus, Ohio, USA

Haemophilus ducreyi causes the sexually transmitted disease chancroid and a chronic limb ulceration syndrome in children. In humans, *H. ducreyi* is found in an abscess and overcomes a hostile environment to establish infection. To sense and respond to membrane stress, bacteria utilize two-component systems (TCSs) and extracytoplasmic function (ECF) sigma factors. We previously showed that activation of CpxRA, the only intact TCS in *H. ducreyi*, does not regulate homologues of envelope protein folding factors but does downregulate genes encoding envelope-localized proteins, including many virulence determinants. *H. ducreyi* also harbors a homologue of RpoE, which is the only ECF sigma factor in the organism. To potentially understand how *H. ducreyi* responds to membrane stress, here we defined RpoE-dependent genes using transcriptome sequencing (RNA-Seq). We identified 180 RpoE-dependent genes, of which 98% were upregulated; a major set of these genes encodes homologues of envelope maintenance and repair factors. We also identified and validated a putative RpoE promoter consensus sequence, which was enriched in the majority of RpoE-dependent targets. Comparison of RpoE-dependent genes to those controlled by CpxR showed that each transcription factor regulated a distinct set of genes. Given that RpoE activated a large number of genes encoding envelope maintenance and repair factors and that CpxRA represses genes encoding envelope-localized proteins, these data suggest that RpoE and CpxRA appear to play distinct yet complementary roles in regulating envelope homeostasis in *H. ducreyi*.

*H*aemophilus ducreyi is a Gram-negative, obligate human pathogen that causes chancroid. Chancroid is a sexually transmitted genital ulcer disease that presents as painful genital ulcers, often associated with regional lymphadenopathy. Chancroid is prevalent in the developing countries of Africa, Asia, and Latin America. Although the global prevalence of chancroid was estimated to be 4 to 6 million cases in the late 1990s, it is now undefined due to syndromic management of genital ulcer disease and the lack of surveillance programs (1, 2). In addition to causing its own morbidity, chancroid facilitates the acquisition and transmission of human immunodeficiency virus type 1 by providing a portal of viral entry, promoting viral shedding from the ulcer, and increasing viral replication due to immune activation (1, 2). Recent reports from the South Pacific islands implicate *H. ducreyi* as a predominant cause of a chronic limb ulceration syndrome in children, which is not sexually transmitted (3–6).

H. ducreyi is thought to enter the skin through abrasions that occur during intercourse. Clinical disease is often characterized initially by a papule at the site(s) of entry. The papules eventually develop into pustules, which finally erode into painful ulcers. To understand how *H. ducreyi* causes infection in its natural host, our laboratory developed a human challenge model of infection (7). In this model, healthy adult volunteers are inoculated with *H. ducreyi* on the skin of the upper arm via puncture wounds. Within 24 h of inoculation, neutrophils and macrophages traffic into the wound and coalesce into an abscess that eventually erodes the epidermis. During both experimental and natural infection, *H. ducreyi* is surrounded by neutrophils and macrophages, which fail to ingest the organism (8, 9). To successfully establish infection in its host, *H. ducreyi* must be able to sense and respond to the hostile environment of an abscess, including toxic products released by phagocytes and epithelial cells, the bactericidal activity of serum that transudates into the wound, hypoxia, and nutrient limitation.

Gram-negative bacteria frequently utilize two-component systems (TCSs) to sense and respond to extracellular stresses. The *H. ducreyi* genome encodes homologues of CpxRA, which is the only obvious intact TCS encoded in the genome. Activation of CpxR by deletion of *cpxA* downregulates the majority of its targets, including multiple virulence determinants, and attenuates the virulence of *H. ducreyi* in humans (10–12). However, deletion of *cpxR* does not affect the expression of virulence determinants or reduce the virulence of the organism in humans, suggesting that CpxRA is dispensable for *H. ducreyi* infection (13). Thus, *H. ducreyi* likely utilizes alternative mechanisms to sense and respond to extracellular stresses *in vivo*.

Gram-negative bacteria also utilize extracytoplasmic function (ECF) sigma factors to sense and respond to extracellular stresses; the *Escherichia coli* RpoE is one of the best-characterized ECF sigma factors. RpoE allows *E. coli* to sense and respond to stresses that perturb the cell envelope (14–17). In the absence of stress, RpoE is bound to the cytoplasmic domain of RseA, an anti-sigma factor, and to RseB, another negative regulator of RpoE (18, 19). RseC is a minor positive regulator of RpoE (19). RpoE is activated

4012 jb.asm.org
Journal of Bacteriology p. 4012–4025
December 2014 Volume 196 Number 23

TABLE 1 Bacterial strains and plasmids used in this study

Strain or plasmid	Description	Source or reference
H. ducreyi strain 35000HP	Human-passaged variant of strain 35000; parental strain	41
E. coli strains		
DH5α and TOP10	Strains used for general cloning procedures	Invitrogen
DY380	DH10B derivative containing a defective λ prophage in which the *red*, *bet*, and *gam* genes are controlled by the temp-sensitive λ*cI*857 repressor	29
Plasmids		
pT	pLS88 derivative containing the tetracycline (*tet*) controlled expression system	27
pDG8	pT derivative containing *rpoE* under control of the *tet* system	This study
pSPECR	Vector containing the spectinomycin resistance cassette	28
pDG9	pT derivative containing the *rpoE* coding region and spectinomycin resistance cassette from pSPECR	This study
pDG10	pT derivative containing the spectinomycin resistance cassette from pSPECR	This study
pDG11	pT derivative containing a 3×-FLAG-tagged RpoE and a spectinomycin resistance cassette	This study
pRB157	pLS88 derivative containing an ΩAmp cartridge followed by a BglII site for insertion of putative promoter sequences and a promoterless GFP cassette derived from pGreenTIR	10
pDG12	pRB157 derivative containing the putative *dsbA* promoter region	This study
pDG13	pRB157 derivative containing the putative *degP* promoter region	This study
pDG14	pRB157 derivative containing the putative *hfq* promoter region	This study
pDG15	pRB157 derivative containing the putative *rpoE* promoter region	This study
pDG16	pRB157 derivative containing the putative *rpoH* promoter region	This study
pLS88	*H. ducreyi* shuttle vector	42
pACYC177	Low-copy-number *H. ducreyi* shuttle vector with a P15A origin of replication	New England Biolabs
pDG17	pACYC177 derivative containing the tetracycline-regulated RpoE expression system	This study
pKF1	pRB157 derivative containing the putative *lspB* promoter region	10
pDG18	pDG16 derivative in which the first putative RpoE-dependent promoter is mutagenized from AAC to TTT at the −35 region	This study
pDG19	pDG16 derivative in which the second putative RpoE-dependent promoter is mutagenized from AAC to TTT at the −35 region	This study

primarily by stresses that affect the folding of outer membrane proteins (OMPs), such as heat shock, oxidative stress, starvation, hyperosmotic stress, exposure to ethanol and detergents, and mutations in genes encoding chaperones for protein folding (20). In the presence of stress stimuli, the carboxyl ends of misfolded OMPs activate the protease activity of DegS, which in turn cleaves RseA in concert with RseP, ClpP, and other proteases, activating the RpoE regulon. Both OMP activation of DegS and lipopolysaccharide (LPS)-dependent relief of RseB inhibition are required for robust induction of RpoE (21, 22). One of the major subsets of genes regulated by RpoE encodes proteins involved in maintenance and repair of the cell envelope (23, 24). RpoE also regulates a number of cytoplasmic proteins involved in transcription, translation, and DNA synthesis and repair. RpoE is an essential sigma factor in *E. coli*; mutations in *rpoE* are either lethal or associated with suppressor mutations (25, 26).

The *H. ducreyi* genome (GenBank accession no. AE017143) contains homologues of RpoE, RseA, RseC, DegS, and RseP. RpoE is the only obvious ECF sigma factor in *H. ducreyi*. Our efforts to generate *rpoE*, *rseA*, and *rseC* mutants of *H. ducreyi* were unsuccessful. As an alternative approach to understand the role of the RpoE-mediated response in *H. ducreyi*, here we defined the genes regulated by RpoE using transcriptome sequencing (RNA-Seq). To this end, we compared the RNA-Seq-defined transcriptome of an *H. ducreyi* 35000HP wild-type strain containing an *rpoE* inducible plasmid to that of a wild-type strain containing a control plasmid. We show that RpoE differentially regulated ~10% of the *H. ducreyi* genes, 98% of which were upregulated. Comparison of

RpoE-dependent genes to those regulated by activated CpxR showed that the two transcription factors regulated unique sets of genes. While CpxRA represses the majority of its targets encoding envelope-localized proteins, RpoE activated a large number of genes involved in envelope maintenance and repair, suggesting that the two systems appear to play distinct yet complementary roles in regulating envelope homeostasis.

MATERIALS AND METHODS

Bacterial strains and culture conditions. The bacterial strains and plasmids used in this study are listed in Table 1. The *H. ducreyi* strains were grown on chocolate agar plates supplemented with 1% IsoVitaleX at 33°C with 5% CO_2 or in Columbia broth supplemented with 5% tetracycline-free fetal bovine serum (Clontech), 1% IsoVitaleX, and 50 μg/ml of hemin (Aldrich Chemical Co.) at 33°C. *E. coli* strain DH5α and One Shot Top10 chemically competent cells (Invitrogen) were used for general cloning purposes. *E. coli* strains were grown in Luria-Bertani medium at 37°C, except for strain DY380, which was maintained in L-broth or L-agar and grown at 32°C or 42°C for induction of the λ red recombinase. When necessary, media were supplemented with spectinomycin (200 μg/ml for *H. ducreyi* and 50 μg/ml for *E. coli*), kanamycin (20 μg/ml for *H. ducreyi* and 50 μg/ml for *E. coli*), and/or streptomycin (100 μg/ml for *H. ducreyi* and 50 μg/ml for *E. coli*).

Construction of a tetracycline-inducible RpoE expression vector. To construct a tetracycline-responsive RpoE expression vector, the *rpoE* coding region was amplified using primers P1/P2 (see Table S1 in the supplemental material), which generated an NdeI site at the 5′ end and a BamHI site at the 3′ end of *rpoE*. The amplified fragment was ligated into NdeI- and BamHI-digested pT, which contains a tetracycline-inducible regulatory system (27); the resulting construct was designated pDG8. Pre-
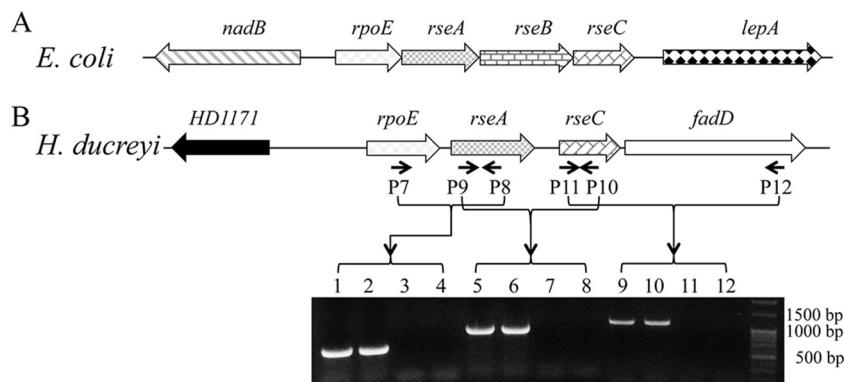
FIG 1 The *rpoE* loci in *E. coli* and *H. ducreyi*. (A) Genomic organization of the *rpoE* locus in *E. coli* K-12. (B) Genomic organization and RT-PCR analysis of the *rpoE* locus in *H. ducreyi*. Arrows indicate the binding sites for primers used for RT-PCR analysis. Lanes 1, 2, 3, and 4, RT-PCR with primers P7 and P8; lanes 5, 6, 7, and 8, RT-PCR with primers P9 and P10; lanes 9, 10, 11, and 12, RT-PCR with primers P11 and P12. Lanes 1, 5, and 9, positive control using genomic DNA; lanes 2, 6, and 10, RT-PCR; lanes 3, 7, and 11, control without reverse transcriptase; lanes 4, 8, and 12, control without template. The RT-PCR data are representative of cDNA made from three independent RNA samples.

liminary experiments showed that 35000HP transformed with pDG8 had severe growth defects in broth, raising the possibility that RpoE was over-expressed in the absence of induction. To reduce the basal level of expression of RpoE, a 1.2-kb spectinomycin cassette from pSPECR was digested with BamHI and ligated in the orientation opposite to that of *rpoE* into BamHI-digested pDG8, generating pDG9 (28). The growth of 35000HP transformed with pDG9 was identical to that of 35000HP (data not shown). As a control, a plasmid that contained all features of pDG9 but lacked *rpoE*, designated pDG10, was also constructed. All constructs were confirmed by sequencing. pDG9 and pDG10 were transformed into *H. ducreyi* 35000HP, and the resulting strains were designated 35000HP-(pDG9) and 35000HP(pDG10), respectively.

A FLAG-tagged RpoE expression vector was constructed by engineering a 3×-FLAG tag sequence into *rpoE* immediately after its translation start codon in pDG9 using λ red recombinase. Briefly, pDG9 was transformed into the *E. coli* strain DY380, which contains the temperature-sensitive λ red recombinase (29). A 150-bp cassette was amplified by PCR using primers P3/P4 (see Table S1 in the supplemental material) with P3 containing the engineered 3×-FLAG tag sequence. The amplified fragment was electroporated into DY380. Following induction of λ red recombinase, the 3×-FLAG tag sequence was inserted immediately downstream of the *rpoE* translation start codon. The resulting construct was designated pDG11 and was confirmed by sequencing using primers P5/P6. pDG11 was transformed into *H. ducreyi* 35000HP, and the resulting strain was designated 35000HP(pDG11).

RT-PCR and qRT-PCR. Total RNA was extracted from bacterial cells using TRIzol reagent (Invitrogen) according to the manufacturer's protocol. To remove DNA, the RNA was treated twice with the Turbo DNase-free DNase (Ambion). The integrity and the concentration of the RNA were determined using the Agilent 2100 Bioanalyzer (Agilent Technologies) and the NanoDrop ND-1000 spectrophotometer (Thermo Scientific), respectively. cDNA was synthesized from total RNA using the Super Smart cDNA synthesis kit (Clontech); reverse transcriptase PCR (RT-PCR) analysis of *rpoE-rseA*, *rseA-rseC*, and *rseC-fadD* was performed using primers P7/P8, P9/P10, and P11/P12, respectively (see Table S1 in the supplemental material).

Quantitative RT-PCR (qRT-PCR) was performed using the QuantiTect SYBR green RT-PCR kit (Qiagen) in an ABI Prism 7000 sequence detection system (Applied Biosystems). qRT-PCR was performed to amplify internal gene-specific fragments ranging from 70 to 200 bp of *HD0518*, *rluA*, *dsbA*, *degP*, and *HD0192* using primers P13/P14, P15/P16, P17/P18, P19/P20, and P21/P22, respectively (see Table S1 in the supplemental material); qRT-PCR analysis of *HD0430*, *HD0930*, *hfq*, and *ompP2B* was performed using primers described

previously (11). The amplification efficiency was determined for each primer pair; all primer pairs had greater than 95% efficiency. The expression levels of target genes were normalized to that of *dnaE* using primers described previously (11). The fold change in expression was calculated as $(E_{\text{target}})^{\Delta CT\text{target} [35000\text{HP}(\text{pDG9}) \, - \, 35000\text{HP}(\text{pDG10})]}/ (E_{\text{reference}})^{\Delta CT\text{reference} [35000\text{HP}(\text{pDG9}) \, - \, 35000\text{HP}(\text{pDG10})]}$, where E is the amplification efficiency (equal to $10^{-1/\text{slope}}$) and ΔC_T is the change in cycle threshold (10).

RpoE induction. 35000HP(pDG9) and 35000HP(pDG10) were grown to mid-log phase (optical density at 660 nm [OD_{660}] = 0.2) and induced for RpoE expression by adding 200 ng/ml of anhydrotetracycline (ATc) (Clontech). To determine if RpoE induction affected *H. ducreyi* growth and viability, OD_{660} and CFU were measured at different time points after induction. *rpoE* transcripts were quantified from 35000HP-(pDG9) and 35000HP(pDG10) cells harvested before and 5, 10, and 20 min after induction by qRT-PCR.

For induction of FLAG-tagged RpoE expression, 35000HP(pDG11) and 35000HP(pDG10) were grown to mid-log phase (OD_{660} = 0.2) and then treated with 200 ng/ml of ATc, harvested, and analyzed as described above. Western blotting was performed on whole-cell lysates of 35000HP-(pDG11) and 35000HP(pDG10) before and 5, 10, and 20 min after adding ATc, using the monoclonal anti-FLAG M2 antibody (Sigma) (11).

RNA-Seq analysis and identification of RpoE-dependent genes. RNA samples were isolated from 35000HP(pDG9) and 35000HP(pDG10) before and 5 and 10 min after induction of *rpoE*. RNA quality and quantity assessment, mRNA enrichment, preparation of RNA-Seq libraries, sequence mapping, quantification of transcript levels, and identification of differentially expressed genes were performed as described previously (11). Sequence was obtained as 50-bp single-end reads on an Illumina HiSeq 2500 instrument. Since *rpoE* transcription was induced during the experiments, *rpoE* transcript levels were excluded from the analysis. Functional classification and clustering analysis of the differentially expressed genes were performed using DAVID bioinformatics resources (30).

Identification of putative RpoE promoter motifs upstream of induced transcriptional units. Putative RpoE promoter motifs were identified *de novo* using the Multiple EM for Motif Elicitation (MEME) algorithm (31). Briefly, the differentially regulated genes were organized into transcriptional units (TUs) using the predicted operon structures from the DOOR database (32). Transcription start sites (TSSs) were predicted for the differentially regulated TUs using the RNA-Seq data. The 100-bp upstream regions from the predicted TSSs were used for *de novo* motif identification by the MEME algorithm, restricting the motif length to 15 to 50 bp. The identified motif was then represented as a position-specific scoring matrix (PSSM). The significance of the discovered motif was
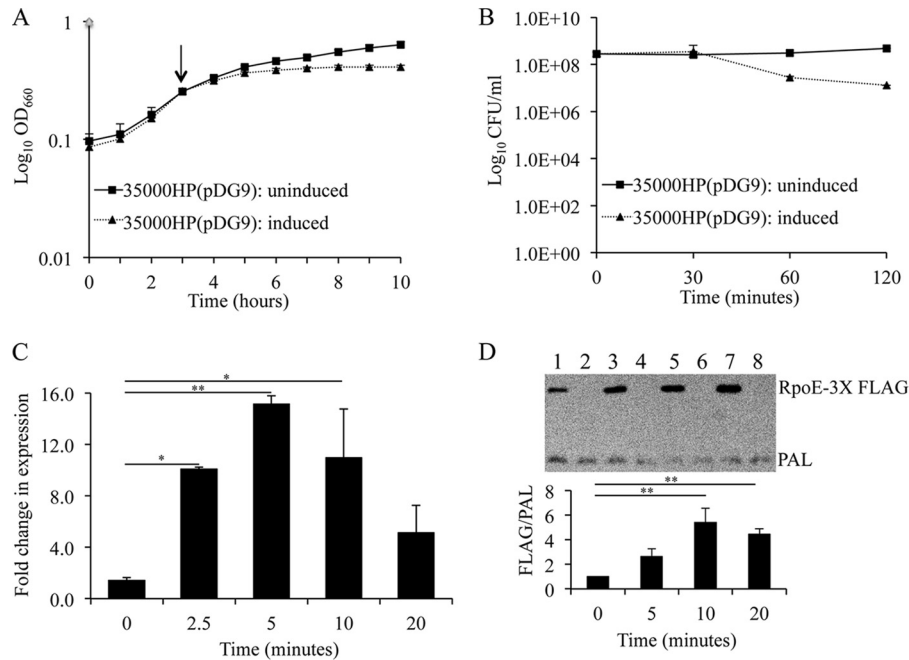
FIG 2 RpoE overexpression using a tetracycline-responsive expression system. (A) Effect of RpoE induction on the growth of 35000HP(pDG9) as assessed by OD measurements at 660 nm. An arrow indicates the point at which ATc was added to induce RpoE expression. (B) Effect of RpoE induction on the viability of 35000HP(pDG9) as assessed by quantitative culture. (C) RpoE induction as assessed by qRT-PCR analysis of *rpoE* transcripts following addition of ATc. (D) RpoE induction as assessed by Western blotting of RpoE expression following addition of ATc. Whole-cell lysates were prepared from 35000HP(pDG11) (lanes 1, 3, 5, and 7) and 35000HP(pDG10) (lanes 2, 4, 6, and 8) at 0, 5, 10, and 20 min after RpoE induction. RpoE expression was determined using a monoclonal antibody specific to the 3×-FLAG tag fused to the N-terminal end of RpoE immediately after the start codon. PAL, detected using the 3B9 antibody, served as a loading control. The data represent the means ± SD from four independent experiments. *, $P < 0.05$ and **$P < 0.01$.
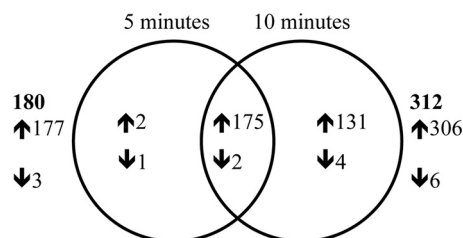
tested by calculating the matching scores based on the putative promoter sequence and the motif feature characterized by the PSSM, using a published strategy (33). The score cutoff was determined by maximizing the enrichment of identified motifs in the putative promoter regions of differentially regulated TUs compared to those of the unaffected genes.

Reporter assays. Reporter assays were performed as previously described (11). Approximately 450-bp upstream regions from the translation start codon containing the putative promoter regions of *dsbA*, *degP*, *hfq*, *rpoE*, and *rpoH* were amplified by PCR using primers P23/P24, P25/P26, P27/P28, P29/P30, and P31/P32, respectively (see Table S1 in the supplemental material). The fragments were ligated to pRB157 using the BglII restriction site preceding a promoterless green fluorescent protein (GFP) gene cassette (34). The orientation of the insert with respect to the GFP gene cassette was confirmed by PCR using a promoter-specific forward primer and the reverse primer that hybridizes to a region of the GFP

FIG 3 Venn diagram showing the overlap in genes differentially expressed at 5 and 10 min after induction of RpoE expression. The up- and downregulated genes are indicated by ↑ and ↓, respectively. The total number of differentially expressed genes at each time point is indicated in bold. 5 min and 10 min, genes differentially expressed in 35000HP(pDG9) relative to 35000HP-(pDG10) at 5 and 10 min after RpoE induction, respectively.

gene cassette downstream of the BglII site described previously (11). The final constructs, designated pDG12, pDG13, pDG14, pDG15, and pDG16, containing the respective putative promoter regions from *dsbA*, *degP*, *hfq*, *rpoE*, and *rpoH* were confirmed by sequencing.

Given that the reporter constructs and the *rpoE* inducible expression system (pDG9) both contained a pLS88 origin of replication, we replaced the pLS88 origin of replication in pDG9 with a p15A origin of replication from pACYC177. Briefly, the regions containing the origin of replication and the ampicillin resistance cassette in pACYC177 and the *rpoE* inducible expression system, including the terminators on either side in pDG9, were amplified using primers P33/P34 and P35/P36, respectively (see Table S1 in the supplemental material). The two fragments were assembled together using the Gibson Assembly cloning kit (New England BioLabs). After confirmation by sequencing, the final construct, designated pDG17, was electroporated into *H. ducreyi* 35000HP, resulting in 35000HP-(pDG17). The growth of 35000HP(pDG17) in broth was identical to that of 35000HP (data not shown). The reporter constructs were then electroporated into 35000HP(pDG17). As a control, a reporter containing the putative *lspB* promoter region was also electroporated into 35000HP-(pDG17) (10). Whole-cell lysates were prepared from each transformant harvested at 0, 30, 60, and 120 min after RpoE induction and analyzed by Western blotting using monoclonal antibodies specific to GFP (Clontech) and the peptidoglycan-associated protein (PAL) (10). For each strain, the level of expression of GFP protein normalized to PAL was determined by densitometry using ImageJ software (35).

Site-directed mutagenesis of putative RpoE-dependent *rpoH* promoter elements. Mutations were introduced into the putative RpoE-dependent *rpoH* promoter region in pDG16 using the QuikChange II XL site-directed mutagenesis kit (Agilent Technologies) following the manufacturer's instructions. The upstream region of *rpoH* in pDG16 contains two putative RpoE-dependent promoters. The third, fourth, and fifth conserved nucleotides in the −35 conserved region of each putative pro-

TABLE 2 Functional classification of genes/open reading frames differentially expressed by overexpression of RpoE in *H. ducreyi*

Regulation and function	No. of genes[a]	
	5 min	10 min
Total differentially expressed genes	180 (98% upregulated, 2% downregulated)	312 (98% upregulated, 2% downregulated)
Upregulated genes		
Envelope		
Lipooligosaccharide biosynthesis and export	13	21
Outer membrane protein assembly and insertion	4	4
Peptidoglycan metabolism	10	13
Periplasmic chaperones and folding catalysts	5	5
Pilus	—[b]	4
Other envelope components	9	10
Cytoplasm		
DNA mismatch repair	8	17
RNA modification	8	10
Regulation of gene expression	12	13
Cofactor biosynthesis	7	14
Amino acid biosynthesis	1	3
Monosaccharide metabolism	1	5
Stress adaptation	3	3
Miscellaneous	1	2
Hypothetical proteins	95	182
Downregulated genes		
Envelope	1	4
Cytoplasm	1	1
Hypothetical proteins	1	1

[a] Number of genes differentially expressed in 35000HP(pDG9) compared to 35000HP(pDG10) at 5 or 10 min after induction of RpoE.
[b] —, no genes were found to be differentially expressed.

moter were mutated from A to T, A/C to T, and C to T, respectively (see Fig. 7A). Mutagenic primers were designed using the QuikChange Primer Design program (Agilent Technologies). The primers P37/P38 and P39/P40 were used to mutagenize putative promoter 1 and 2 regions, respectively; the mutagenized constructs were designated pDG18 and pDG19 (see Table S1 in the supplemental material). The mutations in pDG18 and pDG19 were confirmed by sequencing. The mutagenized constructs were used to transform 35000HP(pDG17); the transformants were grown to mid-log phase and induced for *rpoE* expression, and the expression ratio of GFP/PAL was measured as described above.

Statistical analyses. Densitometry data were analyzed using one-way analysis of variance (ANOVA) with Tukey's honestly significant difference *post hoc* test; a *P* value of <0.05 was considered statistically significant. The overlap of RpoE-dependent genes with those regulated by CpxRA, Hfq, and stationary phase was analyzed using Fisher's exact test; the overlap was considered significant if the odds ratio was >1 and the *P* value was <0.05. Throughout, the data are expressed as means ± standard deviations (SD).

RESULTS

Identification and characterization of the *rpoE* locus in *H. ducreyi*. The *H. ducreyi* genome contains putative homologues of *rpoE* (HD1172), *rseA* (HD1173), *rseC* (HD1174), *degS* (HD1350), *rseP* (HD1192), and *clpP* (HD0221). However, *H. ducreyi* lacks an obvious homologue of *rseB*. By BLAST analysis, the *H. ducreyi* RpoE, RseA, RseC, DegS, RseP, and ClpP had 69%, 32%, 35%, 51%, 43%, and 73% amino acid identity to their respective homologues in *E. coli*. In *E. coli*, *rpoE*, *rseA*, *rseB*, and *rseC* are organized together in an operon (Fig. 1A) (19). The *H. ducreyi rpoE*, *rseA*, and *rseC* genes are also organized in a putative operon with gene order *rpoE*→*rseA*→*rseC*→*fadD* (Fig. 1B); *fadD* is a pseudogene in

H. ducreyi. RT-PCR analysis suggested that *rpoE* is cotranscribed with its downstream genes (Fig. 1B).

Induction of RpoE expression. In *E. coli*, RpoE overexpression has been used to define RpoE-dependent genes (23). *H. ducreyi* RpoE was overexpressed under the control of a tetracycline (*tet*) regulatory system. Compared to uninduced 35000HP(pDG9), 35000HP(pDG9) induced with ATc lagged in growth at 1 h after RpoE induction (Fig. 2A). By quantitative culture, the viability of 35000HP(pDG9) induced for RpoE expression was identical to that of uninduced 35000HP(pDG9) at 30 min but declined by 1.1 ± 0.16 log and 1.4 ± 0.2 log units at 1 and 2 h after induction, respectively (Fig. 2B). These data suggested that RpoE induction needed to be confined to less than 30 min to avoid confounding effects on cell viability. Next, we compared *rpoE* transcripts in 35000HP(pDG9) and 35000HP(pDG10) before and at 2.5, 5, 10, and 20 min after addition of ATc. qRT-PCR analysis showed that *rpoE* was significantly induced at 2.5 (10.1-fold ± 0.1-fold), 5 (15.1-fold ± 0.7-fold), and 10 (11.0-fold ± 3.8-fold) minutes after addition of ATc, with maximal induction at 5 min (Fig. 2C).

In order to confirm that induction of *rpoE* led to increased expression of RpoE, we constructed a FLAG-tagged version of *rpoE* in the plasmid pDG11. In terms of *rpoE* transcription, growth, and viability, 35000HP(pDG11) induced for RpoE expression behaved identically to 35000HP(pDG9) (data not shown). Compared to its vector control [35000HP(pDG10)], Western blot analysis of 35000HP(pDG11) using an anti-FLAG antibody showed that RpoE expression was significantly induced at 10 (5.4-fold ± 1.1-fold) and 20 (4.4-fold ± 0.4-fold) minutes after addition of ATc (Fig. 2D).

TABLE 3 Genes differentially expressed by overexpression of RpoE in *H. ducreyi*

		5 min		10 min	
Function and gene	Description of product	Fold change[a]	*P* value	Fold change[a]	*P* value
Upregulated genes					
Envelope					
Lipopolysaccharide biogenesis and export[b]					
neuA[c]	CMP *N*-acetylneuraminic acid synthetase			2.0	5.5E−21
lst	Lipooligosaccharide sialyltransferase			2.3	3.3E−22
lsgA[c]	Putative lipopolysaccharide biosynthesis protein	3.0	9.3E−40	4.3	2.4E−86
lsgD	Possible lipooligosaccharide n-acetylglucosamine glycosyltransferase	2.8	5.3E−44	4.7	1.4E−107
lsgE	Putative lipooligosaccharide galactosyltransferase	2.0	1.2E−21	3.8	9.0E−81
lsgF	Putative lipooligosaccharide galactosyltransferase	2.0	5.4E−19	3.9	6.4E−76
lgtB	Lipooligosaccharide galactosyltransferase II	3.8	2.9E−24	4.9	3.7E−50
waaF	ADP-heptose-lipooligosaccharide heptosyltransferase II	3.9	5.0E−61	6.7	3.6E−142
lpxL	Lipid A acyltransferase			2.3	1.9E−32
lpxH	UDP-2,3-diacylglucosamine hydrolase			2.2	3.5E−23
lpxD	UDP-3-*O*-(3-hydroxymyristoyl) glucosamine *N*-acyltransferase			2.6	4.6E−36
lpxA	UDP-*N*-acetylglucosamine *O*-acyltransferase			2.1	5.6E−24
gcp	Putative sialylglycoprotease	2.5	4.8E−28	3.3	1.8E−56
fabZ	(3*R*)-Hydroxymyristoyl-acyl carrier protein dehydratase			2.5	2.6E−33
galE	UDP-glucose-4-epimerase	2.2	5.0E−21	3.3	1.1E−56
rmlB[c]	dTDP-D-glucose 4,6-dehydratase			2.1	2.9E−23
glmM[c]	Phosphoglucosamine mutase	3.2	1.0E−50	5.2	4.4E−115
ftsH	Cell division protein FtsH	2.5	5.5E−31	3.8	2.7E−75
HD0552	Lipopolysaccharide export system permease protein	3.1	2.1E−43	4.8	5.2E−99
HD0553	Lipopolysaccharide export system permease protein	2.6	1.9E−34	3.7	3.5E−77
HD0586	Lipopolysaccharide export system ATP-binding protein	2.7	3.1E−30	3.8	1.5E−69
Outer membrane protein assembly and insertion					
D15/bamA	Outer membrane protein D-15	2.5	1.4E−28	4.3	1.2E−82
smpA/bamE	Small protein A	8.4	1.0E−130	15.0	8.0E−252
lpp[c]	15-kDa outer membrane lipoprotein	7.0	1.9E−117	10.8	2.4E−212
lolA	Outer membrane lipoprotein carrier protein	6.3	6.2E−132	11.6	1.0E−257
Peptidoglycan metabolism					
murA	UDP-*N*-acetylglucosamine-1-carboxyvinyltransferase	3.5	2.1E−52	5.7	8.7E−120
ampG	Permease and possible signal transducer AmpG	2.4	4.1E−24	3.8	2.2E−67
ampD	Anhydro-*N*-acetylmuramyl-tripeptide amidase	7.7	4.1E−130	13.9	1.6E−252
uppS[c]	Undecaprenyl pyrophosphate synthetase	8.1	2.1E−133	11.8	8.4E−227
nlpD	Lipoprotein	2.5	3.5E−28	4.8	4.6E−96
prc	Tail-specific protease	3.8	1.0E−66	5.5	4.1E−130
mepA	Penicillin-insensitive murein endopeptidase A			2.5	2.9E−29
dacA	D-Alanyl-D-alanine carboxypeptidase fraction A	2.0	7.6E−26	2.8	3.4E−60
lysA	Diaminopimelate decarboxylase			3.0	2.6E−61
HD0112	*N*-Acetylmuramoyl-L-alanine amidase	2.4	1.1E−04	2.7	1.2E−06
HD0501	*N*-Acetylmuramoyl-acetylmuramoyl-L-alanine amidase			2.6	2.9E−32
HD0922	Hypothetical protein	2.6	9.3E−35	5.4	1.7E−108
HD1339	Hypothetical protein	3.5	6.6E−63	5.1	3.0E−124
Periplasmic chaperones and folding catalysts					
degP	Periplasmic serine protease do	7.8	1.2E−135	13.0	5.2E−249
ecfE	Protease EcfE	3.7	3.9E−55	5.3	1.1E−108
dsbA	Probable thiol:disulfide interchange protein	3.9	8.1E−56	6.3	1.7E−126
surA[c]	Peptidyl-prolyl *cis-trans* isomerase	3.5	5.7E−50	4.3	1.7E−87
dsbC	Thiol:disulfide interchange protein	3.4	7.1E−55	5.3	1.4E−119
Pilus					
fimA[c]	Possible fimbrial major pilin protein			2.4	1.7E−26
fimB	Possible fimbrial structural subunit			2.2	2.4E−17
fimC	Probable fimbrial outer membrane usher protein			2.1	1.1E−19
fimD	Probable periplasmic fimbrial chaperone			2.1	4.2E−20

(Continued on following page)

TABLE 3 (Continued)

Function and gene	Description of product	5 min		10 min	
		Fold change[a]	P value	Fold change[a]	P value
Other envelope components					
hlp	Lipoprotein Hlp	3.0	7.2E−39	3.8	5.3E−72
lspA	Lipoprotein signal peptidase	2.7	1.0E−33	3.9	2.2E−77
yfeB	Iron (chelated) transporter, ATP-binding protein	3.4	8.1E−49	4.4	1.3E−87
cdsA	CDP-diglyceride pyrophosphorylase	6.3	2.7E−108	8.7	8.3E−184
comA[c]	Possible competence protein A-like protein	2.1	1.8E−10	2.8	1.0E−23
HD1126	Leader peptidase HopD			2.1	3.3E−10
HD1820	ABC transporter ATP binding protein	2.5	2.8E−23	3.8	3.6E−62
HD1821	ABC transporter	2.4	2.0E−19	3.6	1.8E−52
oapA	Opacity associated protein A	6.0	4.6E−102	9.9	6.7E−200
oapB	Opacity associated protein B	4.5	4.2E−72	7.4	5.6E−153
Cytoplasm					
DNA mismatch repair					
topB1	DNA topoisomerase III			2.5	1.1E−34
ssb2	Single-stranded DNA-binding protein			2.8	9.3E−27
topB2	DNA topoisomerase III			2.3	7.6E−28
sbcB[c]	Exodeoxyribonuclease I	2.9	1.7E−36	3.9	2.2E−74
trpH	TrpH-like protein			2.3	8.4E−31
dnaX	DNA polymerase III subunits gamma and tau	2.8	3.2E−31	4.1	2.8E−71
holB	DNA polymerase III delta′ subunit	3.1	5.3E−35	4.8	6.5E−88
mutY[c]	A/G-specific adenine glycosylase			2.5	2.3E−44
recJ	Single-stranded-DNA-specific exonuclease RecJ	3.0	2.0E−47	5.2	7.2E−120
gam	Putative mu phage host nuclease inhibitor protein			2.1	2.9E−06
recQ	ATP-dependent DNA helicase			2.0	4.3E−21
uvrD	DNA helicase II	2.2	2.4E−19	3.8	2.5E−66
uvrB	Excinuclease ABC subunit B			2.3	5.4E−29
mutT	7,8-Dihydro-8-oxoguanine-triphosphatase	4.6	1.2E−79	6.9	6.0E−153
apt[c]	Adenine phosphoribosyltransferase	3.7	1.2E−44	5.0	6.3E−89
tmk	Thymidylate kinase	3.4	4.3E−43	5.3	3.6E−102
upp	Uracil phosphoribosyltransferase			3.2	1.2E−59
RNA modification					
trmA[c]	tRNA (uracil-5-)-methyltransferase			2.2	2.1E−31
miaA	tRNA delta-2-isopentylpyrophosphate transferase	4.1	4.2E−62	5.8	6.0E−120
rsuA	Ribosomal small subunit pseudouridine synthase A	3.3	8.7E−57	4.3	3.7E−102
ksgA	Dimethyladenosine transferase	3.0	2.7E−36	3.7	1.8E−67
tgt	tRNA-guanine transglycosylase			2.3	2.0E−27
rluA	Pseudouridylate synthase	4.5	8.9E−71	6.8	1.1E−139
rumB	23S rRNA (uracil-5-)-methyltransferase	3.7	2.0E−42	4.6	8.5E−73
rimK	Ribosomal protein S6 modification protein	6.4	4.7E−116	11.5	2.2E−232
HD1138	tRNA pseudouridine synthase C	2.4	3.6E−28	3.7	3.4E−74
HD1770	Nitrogen regulatory protein	2.0	1.2E−20	2.5	4.9E−41
Regulation of gene expression					
rpoH	RNA polymerase sigma 32 factor	4.5	8.9E−73	6.4	4.4E−135
rseA	Possible sigma E factor negative regulatory protein	4.9	1.5E−79	6.6	5.2E−139
rseC	Possible sigma E factor regulatory protein	2.8	9.0E−40	3.5	3.1E−71
cpxR	Transcriptional regulatory protein CpxR	3.0	1.9E−42	4.3	1.6E−90
cpxA	Sensor kinase CpxA	2.4	1.1E−27	3.2	5.0E−58
ptsN	Phosphotransferase system, nitrogen regulatory IIA-like protein	2.5	4.2E−28	3.8	2.2E−69
hfq	Putative host factor I protein	3.0	1.2E−35	4.1	3.9E−73
glnB	Putative nitrogen regulatory protein P-II	2.6	5.3E−35	3.9	8.0E−83
argR[c]	Arginine repressor			2.3	4.5E−29
asnC	Transcription regulatory protein, AsnC	2.0	4.0E−19	2.6	8.3E−42
cysB	Cys regulon transcriptional activator	4.3	5.7E−75	7.0	3.2E−156
fabR	DNA-binding transcriptional repressor FabR	4.2	2.0E−74	6.6	8.3E−151
Cofactor biosynthesis					
mogA[c]	Molybdopterin biosynthesis protein	2.7	3.2E−38	4.1	2.9E−90
ispH	Hydroxymethylbutenyl pyrophosphate reductase	2.2	5.5E−22	3.4	3.0E−62
visC	Probable monooxygenase			2.7	3.0E−40

TABLE 3 (Continued)

Function and gene	Description of product	5 min		10 min	
		Fold change[a]	P value	Fold change[a]	P value
hemY	HemY protein			2.3	4.8E−40
hemX	Putative uroporphyrinogen III C-methyltransferase			2.2	2.3E−39
modA	Molybdate-binding periplasmic protein			3.1	4.7E−48
modB	Molybdenum ABC transporter, permease protein			2.8	6.2E−41
modC	Molybdenum ABC transporter, ATP-binding protein			2.7	4.7E−39
lipA	Lipoic acid synthetase			3.0	2.3E−58
lipB	Lipoate biosynthesis protein B	2.1	2.3E−27	3.3	8.3E−74
rpiA	Ribose 5-phosphate isomerase A	2.7	1.6E−39	4.9	1.2E−111
mdh	Malate dehydrogenase	3.2	1.0E−41	4.4	2.7E−84
HD0261	Hypothetical protein	3.7	4.6E−53	5.6	4.5E−115
HD1410	Hypothetical protein	2.9	1.1E−35	4.0	1.1E−74
Amino acid biosynthesis					
argH	Arginosuccinate lyase			2.9	4.8E−41
aroC	Chorismate synthase			2.4	2.8E−31
cysZ	Cysteine synthetase	2.8	1.3E−35	4.6	1.1E−89
Monosaccharide metabolism					
pflB	Formate acetyltransferase	2.4	3.7E−34	3.8	4.5E−89
citC	Citrate lyase synthetase			3.6	5.0E−72
citD[c]	Citrate lyase gamma chain			3.1	3.5E−51
citE	Citryl coenzyme A lyase subunit			2.9	6.4E−54
citF	Citrate coenzyme A transferase subunit			2.1	8.2E−26
Stress adaptation					
surE[c]	Acid phosphatase stationary-phase survival protein	5.0	5.0E−90	8.9	2.2E−191
proQ	Possible ProP effector	4.5	3.1E−79	6.1	3.8E−141
mazG[c]	MazG protein	3.1	5.9E−46	4.2	5.6E−88
Miscellaneous					
vacB	RNase R, virulence associated VacB-like protein	2.9	1.2E−33	5.1	4.1E−98
hflX	GTP-binding protein HflX			2.4	4.5E−25
Downregulated genes					
Envelope					
ccmD	Cytochrome *c* maturation protein D			−2.1	2.2E−04
ompA2[c]	Major outer membrane protein-like protein OmpA2			−2.6	2.3E−45
ompP2A	Outer membrane protein P2-like protein			−2.3	1.7E−30
ompP2B	Outer membrane protein P2-like protein	−2.2	8.1E−19	−2.7	5.3E−36
Cytoplasm					
purM	Phosphoribosylformylglycinamidine cyclo-ligase	−2.7	7.0E−10		
pyrE	Orotate phosphoribosyltransferase			−2.1	7.9E−28

[a] Mean fold change in expression of genes in 35000HP(pDG9) compared to 35000HP(pDG10) at 5 or 10 min after induction of RpoE; the fold change was normalized by dividing the fold change at 5 or 10 min with that of 0 min.

[b] Differentially expressed genes were categorized into different functional categories using DAVID bioinformatics resources.

[c] First gene of a known or putative operon predicted by the DOOR database.

Transcriptome analysis. To define RpoE-dependent genes, we compared the transcriptome of the RpoE-overexpressing strain [35000HP(pDG9)] to that of its vector control [35000HP-(pDG10)]. We grew the strains to mid-log phase, induced their expression systems with ATc, isolated RNA, and determined their transcriptomes by RNA-Seq.

To reduce indirect transcriptional changes caused by RpoE overexpression, we harvested cells before and at 5 and 10 min after RpoE induction. Within each strain, fold changes in gene expression levels at 5 and 10 min were determined by comparison to preinduction levels. As described previously, a false-discovery rate (FDR) of ≤0.1 and a fold change of ≥2 were used as criteria for differential transcript expression (11). For each strain and time point, four biological replicates were included, totaling 24 samples (see Table S2 in the supplemental material). The percentage of total reads aligned to the reference genome, the percentage of reads aligned to the coding regions, and the average coverage per nucleotide from all strains and time points ranged from 90.7 to 96.7%, 81.3 to 91.4%, and 5.9 to 10.5, respectively (see Table S2 in the supplemental material). The coefficients of determination (R^2) of gene expression levels between the samples within each time point and strain ranged from 0.98 to 0.99, indicating that the RNA-Seq data were highly reproducible.

Comparison of the transcriptomes of 35000HP(pDG9) and 35000HP(pDG10) yielded 180 and 312 differentially expressed genes at 5 and 10 min after RpoE induction, respectively; of these, 98.3% and 98% were upregulated (Fig. 3 and Tables 2 and 3; see Table S3 in the supplemental material). Of the 180 and 312 differentially expressed genes, 175 were differentially expressed at both time points (Fig. 3). Since it was possible that some of the tran-
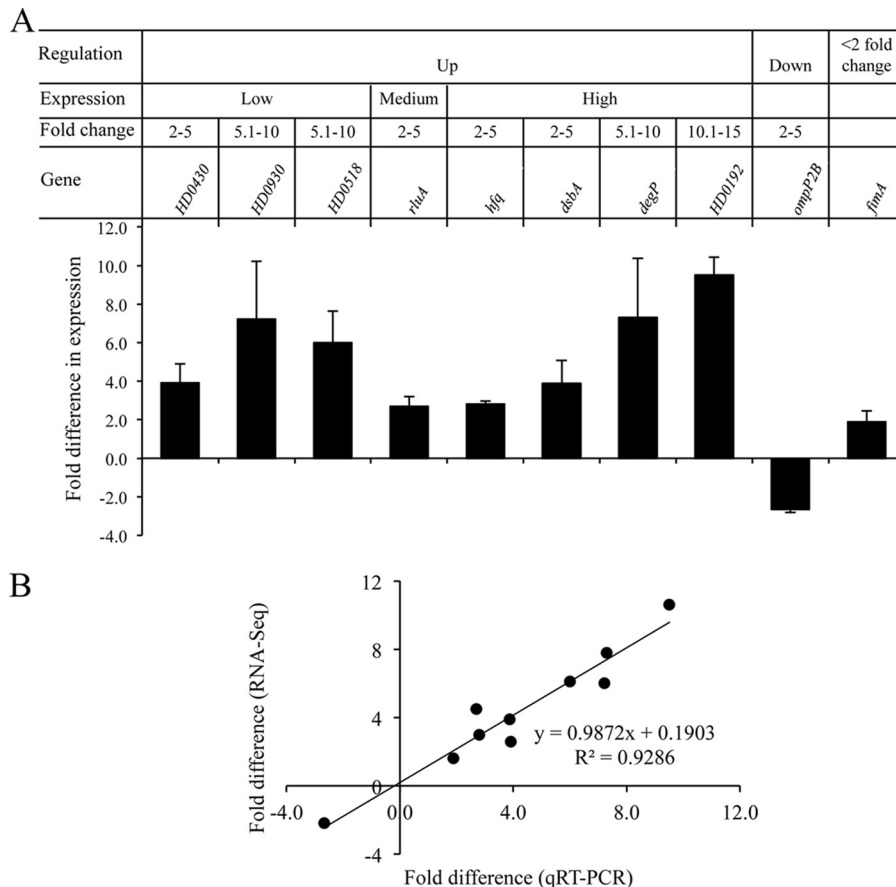
FIG 4 qRT-PCR validation of the RNA-Seq data. (A) Fold change in the expression of target genes in 35000HP(pDG9) relative to 35000HP(pDG10) at 5 min after induction. The criteria used for selecting the targets for qRT-PCR validation are outlined in the figure. The expression levels of target genes were normalized to that of *dnaE*. The data represent the means ± SD from four independent experiments. (B) Correlation between the fold changes derived from qRT-PCR and RNA-Seq.

scriptional effects seen after 10 min of induction were indirect, we focused primarily on transcriptional changes seen after 5 min of induction for the remainder of the study.

qRT-PCR confirms the fold changes determined by RNA-Seq. We validated selected differentially regulated targets using qRT-PCR (11). The targets were first grouped into up- and down-regulated genes (Fig. 4A). The upregulated genes were then sub-grouped based on their expression levels (high, medium, and low) (Fig. 4A). Genes in each expression level were further stratified based on their fold change (2.0 to 5.0, 5.1 to 10.0, and 10.1 to 15.0) (Fig. 4A). Representative genes were selected arbitrarily from each category; a total of 9 genes were evaluated by qRT-PCR. qRT-PCR analysis confirmed the differential expression of 9/9 targets identified by RNA-Seq (Fig. 4A). Fold changes derived from RNA-Seq were in good agreement with those derived from qRT-PCR (Fig. 4B).

***De novo* identification of putative RpoE promoter motifs.** The differentially regulated genes belonged to 73 putative transcriptional units (TUs); transcription start sites (TSSs) were predicted for 44 of these TUs using RNA-Seq data (see Table S4 in the supplemental material). A *de novo* motif analysis of the 100-bp upstream putative promoter regions from the predicted TSSs of the 44 RpoE-dependent TUs identified an RpoE consensus sequence with an expected value of 3.5×10^{-2} (Fig. 5A and B). The

identified sequence logo consisted of a −35 region, a 15- to 17-nucleotide spacer, and a −10 region. The *H. ducreyi* logo was similar to the *E. coli* RpoE consensus sequence, which contains the −35 motif GGAACTT, a 15- to 19-nucleotide spacer, and the −10 motif TCAAA (23).

A genome-wide search using a position-specific scoring matrix (PSSM) derived from the *H. ducreyi* −35 and −10 motifs in the 450-bp upstream and 100-bp downstream regions from the translational start codon showed that this logo was present in the upstream putative promoter sequences of 51 out of 73 (70%) RpoE-dependent TUs and in 326 out of 616 (53%) TUs whose expression levels were not differentially regulated (odds ratio = 2.06; $P < 0.006$) (see Table S5 in the supplemental material). Given that a relatively higher percentage of nondifferentially regulated TUs contained the RpoE promoter motifs, we calculated the random occurrence of the motifs in the *H. ducreyi* genome using Fisher's exact test; the results from this analysis showed that the motif was randomly found in 337 out of 616 (55%) nondifferentially regulated TUs. The percentage of nondifferentially regulated TUs that contained the RpoE motifs by chance (55%) is close to the percentage of nondifferentially regulated TUs that contained the RpoE motifs in our enrichment analysis (53%). Using random occurrence as 55%, the expected occurrence of the predicted motifs in differentially regulated TUs is 40 out of 73. How-
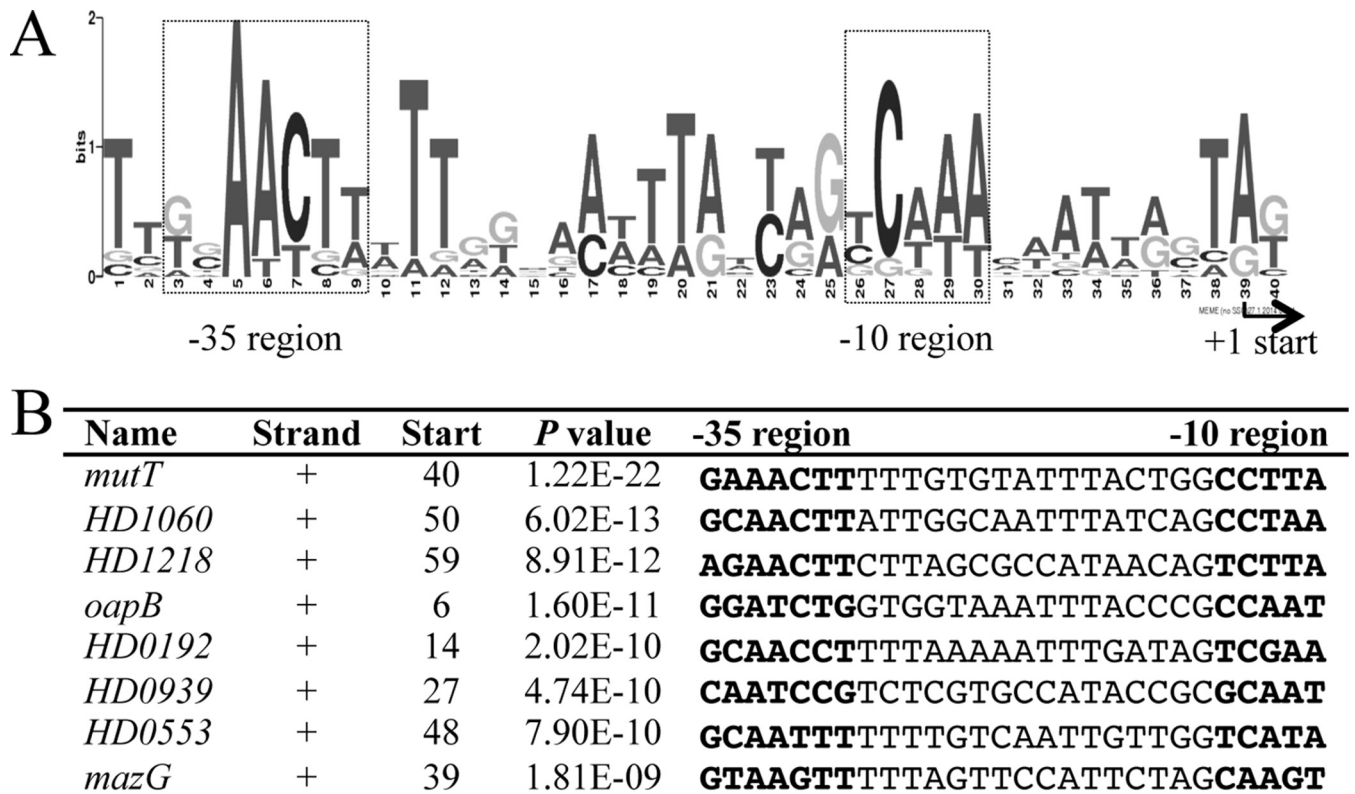
FIG 5 Sequence logo of the *H. ducreyi* RpoE promoter motifs. (A) Sequence logo of the *H. ducreyi* RpoE promoter motifs. The logo was generated by the MEME algorithm using the 100-bp upstream sequences from the TSSs of 44 of 73 RpoE-dependent TUs for which the TSSs could be predicted based on the RNA-Seq data. The putative TSS is indicated, and the putative −10 and −35 regions are boxed. (B) Multiple-sequence alignment of the RpoE promoter region in the eight putative RpoE-dependent promoters that contained the most significant matches. Name, gene in which the motif was identified; Strand, strand in which the gene is located (+, sense strand; −, antisense strand); Start, start position of the binding site relative to the TSS; *P* value, *P* value for the predicted promoter motifs; −35 and −10 regions of the predicted promoter are highlighted in bold.

ever, our enrichment analysis showed that 51 out of 73 differentially regulated TUs contained the RpoE motifs, indicating that the promoter motifs were 27.5% enriched in the differentially regulated TUs compared to those whose expression levels were not differentially regulated. These data suggest that the high occurrence of the RpoE motifs in nondifferentially regulated TUs is likely due to random occurrence of the RpoE promoter motifs in the *H. ducreyi* genome. Our data also suggest that, despite the high random occurrence of the RpoE promoter motifs in the *H. ducreyi* genome, the identified promoter motifs were enriched in RpoE-dependent TUs.

Reporter assays confirm RpoE regulation of putative target promoters. We sought to determine the RpoE dependence of putative target promoters in 35000HP. We constructed reporter plasmids containing the promoter regions of the RpoE targets *dsbA*, *degP*, *hfq*, *rpoE*, and *rpoH*. As a negative control, we used an *lspB* reporter, which lacks the putative RpoE-dependent promoter. The reporters were transformed into 35000HP(pDG17), which contains the *rpoE* inducible system. Overexpression of RpoE from the low-copy-number plasmid pDG17 did not affect the viability of *H. ducreyi* after induction for up to 2 h (data not shown). Therefore, we induced RpoE expression and measured the ratio of GFP protein levels relative to PAL at 0, 30, 60, and 120 min after RpoE induction. Compared to at 0 min, the reporter activity of *dsbA* (60 min, 3.2-fold ± 0.8-fold; 120 min, 6.1-fold ±

1.4-fold), *degP* (60 min, 3.8-fold ± 0.7-fold; 120 min, 8.3-fold ± 1.3-fold), *hfq* (120 min, 2.8-fold ± 0.8-fold), and *rpoH* (30 min, 1.7-fold ± 0.3-fold; 60 min, 2.9-fold ± 0.5-fold; 120 min, 4.3-fold ± 0.4-fold) significantly increased after induction, confirming RpoE regulation of these targets (Fig. 6A and B). As expected, the activity of an *lspB* reporter did not increase after induction (Fig. 6A and B).

RpoE overexpression increased the transcript levels of *rseA* and *rseC* (Table 2). RT-PCR analysis suggested that *rpoE*, *rseA*, and *rseC* are in an operon (Fig. 1B). Compared to at 0 min, the reporter activity of the putative promoter preceding the *rpoE* TU significantly increased at 120 min after RpoE induction ($P < 0.05$), suggesting that RpoE is autoregulated in *H. ducreyi* (Fig. 6A and B).

Site-directed mutagenesis confirms the predicted RpoE-dependent promoter. The majority of the RpoE-dependent targets contained one or more putative RpoE promoter motifs (see Table S5 in the supplemental material). To validate whether RpoE utilizes the predicted RpoE-dependent promoter motifs to control its targets, we selected the reporter strain containing the putative *rpoH* promoter region. Bioinformatics analysis showed the presence of two putative RpoE-dependent promoter motifs in the putative *rpoH* promoter region (Fig. 7A). To identify which of these motifs was required for RpoE-dependent regulation of *rpoH*, we mutagenized the third, fourth, and fifth nucleotides in the −35
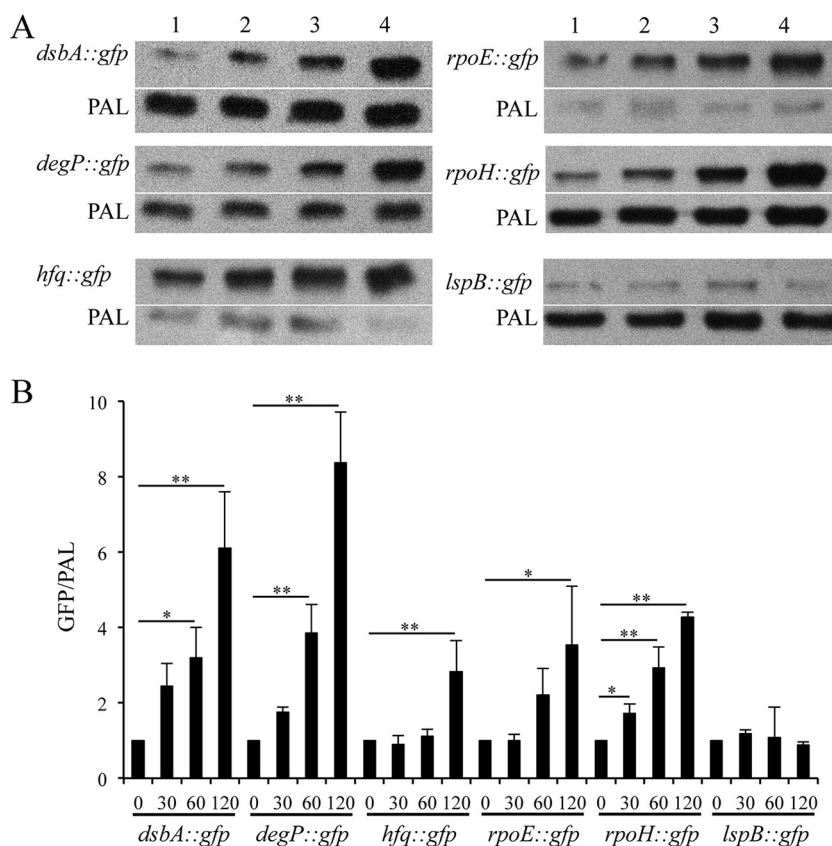
FIG 6 Promoter-reporter analysis of the RpoE-dependent targets identified by RNA-Seq. (A) *In vivo* transcriptional activity of the putative RpoE-dependent promoters at 0 (lane 1), 30 (lane 2), 60 (lane 3), and 120 (lane 4) minutes after RpoE induction. For assessing the promoter activity, whole-cell lysates were prepared from *H. ducreyi* strains containing pDG17 and the reporter constructs at 0, 30, 60, and 120 min after RpoE induction and probed with an anti-GFP monoclonal antibody and anti-PAL monoclonal antibody 3B9, which served as a loading control. (B) Densitometry analysis of the Western blots from panel A. The data represent the means ± SD from three independent experiments. *, $P < 0.05$; **, $P < 0.01$.

regions of the 2 putative promoters (Fig. 7A). Compared to at 0 min, the reporter activity of 35000HP(pDG16)(pDG17), which contains the wild-type putative *rpoH* promoter, significantly increased after RpoE induction (120 min, 3.5-fold ± 1.3-fold) (Fig. 7B and C). Compared to at 0 min, the reporter activity of 35000HP(pDG19)(pDG17), which harbors mutations in the putative promoter 2 region, significantly increased after RpoE induction (60 min, 2.3-fold ± 0.2-fold; 120 min, 3.5-fold ± 0.5-fold) (Fig. 7B and C). However, compared to at 0 min, the reporter activity of 35000HP(pDG18)(pDG17), which harbors mutations in the putative promoter 1 region, was unaltered after RpoE induction (Fig. 7B and C). These data suggest that the putative promoter 1 region is required for RpoE-dependent regulation of *rpoH* and that RpoE likely utilizes the predicted promoter sequence to control its targets (Fig. 5A).

Functional analysis of genes regulated by RpoE. We analyzed the genes that were differentially regulated after 5 and 10 min of induction (Tables 2 and 3). The RpoE-dependent genes belonged to several functional categories; DAVID bioinformatics analyses showed that several pathways or functional clusters were statistically enriched (30). Clusters involved in envelope homeostasis such as those encoding factors involved in LPS biosynthesis and export (*lsgA, lsgD, lsgE, lsgF, lgtB, waaF, glmM, galE, ftsH, HD0552, HD0553,* and *HD0586*), OMP assembly and insertion (*D15/bamA, smpA/bamE, lpp,* and *lolA*), peptidoglycan metabolism

(*murA, ampD, uppS, ampG, nlpD, prc, dacA, HD0112, HD0922,* and *HD1339*), and periplasmic chaperones and folding catalysts (*degP, ecfE, dsbA, surA,* and *dsbC*) constituted a major part of the enriched clusters (Table 3). A second major enriched cluster encoded homologues of factors involved in DNA mismatch repair (*recJ, sbcB, mutT, uvrB, apt, tmk,* and *dnaX*) and RNA modification (*ksgA, rsuA, rluA, miaA, rumB, HD1138,* and *HD1770*) (Table 3). A third major cluster of enriched genes encoded homologues of factors involved in regulation of gene expression (*glnB, cysB, cpxR, cpxA, hfq, rpoH, rseA, rseC, ptsN,* and *asnC*) (Table 3).

Comparison of RpoE-dependent genes to the CpxR and Hfq regulons and genes differentially regulated during stationary phase. We recently defined the genes differentially regulated by CpxR, Hfq, and growth in stationary phase relative to mid-log phase in *H. ducreyi*; we found that Hfq regulates stationary-phase gene expression in *H. ducreyi* (11, 36). Since RpoE overexpression increased the transcription of *cpxRA* and *hfq*, we compared the RpoE-dependent genes to those differentially regulated by CpxR, Hfq, and stationary phase relative to mid-log phase. For this analysis, overlap was defined as differentially regulated genes whose expression was positively correlated (i.e., both upregulated or both downregulated). Compared to a *cpxR* deletion mutant, a *cpxR*-activating mutant differentially regulates approximately 140 genes in *H. ducreyi* harvested from stationary phase. There was no overlap between the 140 genes differentially regulated by CpxR
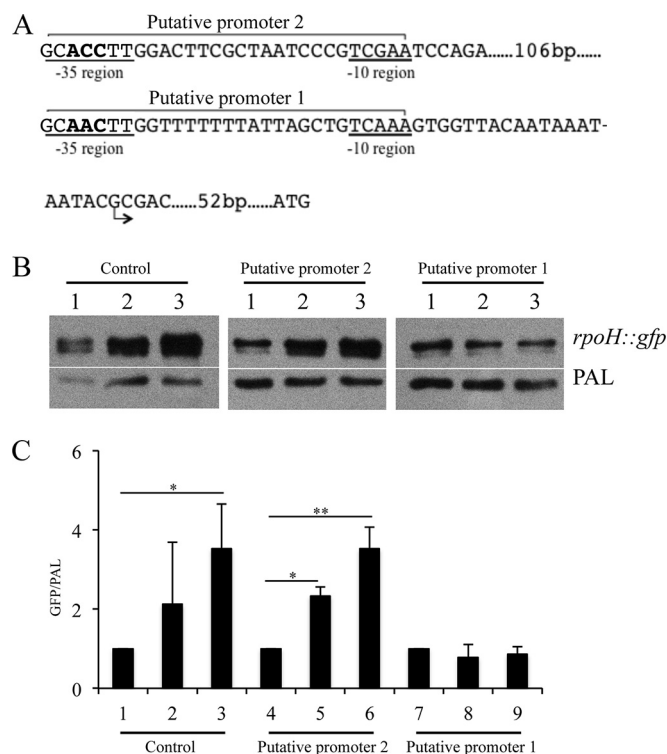
FIG 7 The predicted RpoE promoter is required for RpoE-dependent regulation of *rpoH*. (A) The predicted −10 and −35 regions of the two tandem RpoE-dependent promoters as well as the transcriptional and translational start sites are shown. In order to demonstrate that these promoter regions were functional, we mutagenized nucleotides within each −35 region. The mutagenized nucleotides are indicated in bold. (B) Effect of site-directed mutagenesis on promoter activity measured in the GFP reporter assay. Plasmids containing the wild-type and mutagenized putative *rpoH* promoter regions were electroporated into 35000HP(pDG17). Whole-cell lysates were prepared at 0 (lane 1), 60 (lane 2), and 120 (lane 3) minutes after RpoE induction and probed with an anti-GFP monoclonal antibody. PAL detected with the monoclonal antibody 3B9 served as a loading control. Putative promoter 1 and putative promoter 2, reporters with nucleotide substitutions in each putative promoter; control, reporter containing the wild-type putative *rpoH* promoter region. (C) Densitometry analysis of the Western blots from panel B. The data represent the means ± SD from three independent experiments. *, $P < 0.05$; **, $P < 0.01$.

and the 180 genes differentially regulated by RpoE overexpression. There are approximately 282 Hfq-dependent genes in *H. ducreyi*. There was less overlap of the genes differentially regulated by RpoE overexpression and those regulated by Hfq than was expected by chance (12/180 genes) (odds ratio = 0.35; $P = 0.00015$). Compared to organisms grown to mid-log phase, *H. ducreyi* harvested from stationary phase differentially regulated approximately 288 genes. Considering these 288 genes, there was a significant overlap of 180 genes differentially regulated by RpoE overexpression (46/180 genes) (odds ratio = 1.93; $P = 0.0006$). Taken together, these data suggest that under the conditions tested, the RpoE, CpxRA, and Hfq regulons do not appear to significantly overlap and that RpoE may play a role in stationary-phase gene regulation in *H. ducreyi*.

DISCUSSION

The *H. ducreyi* genome encodes homologues of two systems that generally respond to stresses affecting the cell envelope: RpoE and

CpxRA. We previously showed that activation of CpxRA in *H. ducreyi* represses the majority of its targets encoding envelope-localized proteins, including known virulence determinants, but does not affect the transcription of genes involved in envelope protein folding and chaperoning (11, 12). To potentially understand how *H. ducreyi* regulates envelope stress responses, here we defined RpoE-dependent genes in *H. ducreyi*. We compared the transcriptome of a strain containing a plasmid that can be induced to expresses RpoE to that of a strain containing a vector control. The rationale for this approach is discussed in detail by Rhodius et al., who employed the same strategy to identify RpoE-dependent genes in *E. coli* (23). RpoE overexpression upregulated *cpxRA* and *hfq*, which are also involved in gene regulation in *H. ducreyi* (11, 12, 36). This raised the possibility that some of the transcriptional effects caused by overexpression of RpoE were indirect. Comparison of RpoE-dependent genes to those regulated by CpxR and Hfq showed no or little overlap. All together, these data suggest that the transcriptional changes resulting from RpoE overexpression are more likely due to direct regulation by RpoE and less likely due to secondary activation of other regulatory systems.

We showed that *H. ducreyi* RpoE upregulates 98% of its targets; a large number of these encode factors involved in envelope maintenance and repair. Unlike RpoE, *H. ducreyi* CpxRA downregulates the majority of its targets; most of these encode envelope-localized proteins (11, 12). Thus, RpoE functions primarily to maintain and repair the envelope, while CpxRA functions primarily to reduce protein traffic across the envelope, which otherwise may exacerbate preexisting envelope stress. These data suggest that RpoE and CpxRA appear to play distinct yet complementary roles in regulating envelope homeostasis in *H. ducreyi*.

H. ducreyi lacks a homologue of RpoS, which regulates stationary-phase gene expression in other organisms (37). Compared to mid-log phase, entry into stationary phase is associated with differential regulation of 288 *H. ducreyi* genes (36). Comparison of the genes altered by overexpression of RpoE to those differentially regulated in stationary phase relative to mid-log phase showed that approximately 26% of the genes altered by overexpression of RpoE overlapped and were positively correlated with those differentially regulated in stationary phase relative to mid-log phase (36). Hfq is a major regulator of stationary-phase gene expression in *H. ducreyi* (36). Although RpoE overexpression increased *hfq* transcription, comparison of RpoE-dependent genes to those regulated by Hfq showed little overlap, suggesting that the overlap between RpoE-dependent genes and those upregulated in stationary phase is not due to RpoE-dependent upregulation of *hfq* expression (36). Although not experimentally addressed in this study, the data suggest that RpoE may also play a role in stationary-phase gene regulation in *H. ducreyi*.

One limitation of our study is that we did not define physiological signals that activate RpoE in *H. ducreyi*. We considered using the reporter constructs containing putative RpoE-dependent promoters to study such signals. However, due to our inability to recover an *rpoE* mutant, we did not have an appropriate negative control for these studies. In *E. coli*, RpoE is activated by a variety of envelope-perturbing stresses that lead to misfolded proteins in the outer membrane, upregulates several genes involved in envelope maintenance and repair, and coordinates with other stress response regulators (16, 17, 20, 23). Similarly, *H. ducreyi* RpoE upregulated a large number of genes encoding factors involved in envelope maintenance and repair as well as those encod-

ing several other stress response regulators. Despite the lack of information about the signals that activate RpoE in *H. ducreyi*, our results suggest that RpoE likely controls the response to envelope stress in this organism.

Our inability to obtain an *rpoE* mutant suggests that this ECF sigma factor is likely essential in *H. ducreyi*. A large set of RpoE-dependent genes encodes homologues of factors involved in maintenance or repair of the cell envelope, suggesting that loss of RpoE may lead to loss of envelope integrity. On the other hand, RpoE overexpression was also toxic to *H. ducreyi*. This is perhaps due to redirection of cellular resources away from essential functions toward the synthesis of envelope components. Alternatively, as most RpoE-dependent genes encode homologues of proteins that localize to the periplasm/outer membrane, overexpression of RpoE may lead to saturation of membrane protein translocation machinery, resulting in cellular toxicity. These data underscore the fact that RpoE expression needs to be tightly regulated in order to ensure viability.

In *E. coli*, the CpxRA and RpoE systems are interconnected. For example, both RpoE and CpxRA positively regulate a large number of genes encoding protein folding and chaperoning factors and jointly regulate *degP* (17, 20, 23, 38–40). In *H. ducreyi*, RpoE regulates homologues of these genes, including *degP*, while CpxRA does not. In *E. coli*, activation of CpxRA negatively regulates *rpoE* transcription, and RpoE does not regulate *cpxRA* transcription (20, 23, 38). In contrast, activation of CpxRA does not regulate *rpoE* transcription in *H. ducreyi*, but RpoE positively regulates *cpxRA* transcription (11). Thus, the interconnections between the CpxRA and RpoE systems in *H. ducreyi* differ from those in *E. coli*.

We conclude that *H. ducreyi* RpoE positively regulates a large number of genes involved in envelope maintenance and repair. In addition to its role in envelope homeostasis, our findings also suggest a possible role for RpoE in stationary-phase gene regulation in *H. ducreyi*. Future studies will focus on characterizing the contribution of RpoE-dependent genes to the ability of *H. ducreyi* to survive in humans.

REFERENCES

1. **Spinola SM, Ballard RC.** 2010. Chancroid, p 141–156. *In* Morse SA, Holmes, KK, Ballard, RC (ed), Atlas of sexually transmitted diseases and AIDS, 4th ed. Saunders, Philadelphia, PA.
2. **Spinola SM.** 2008. Chancroid and *Haemophilus ducreyi*, p 689–699. *In* Holmes KK, Sparling PF, Stamm WE, Piot P, Wasserheit JN, Corey L, Cohen MS, Watts DH (ed), Sexually transmitted diseases, 4th ed. McGraw-Hill, New York, NY.
3. **Ussher JE, Wilson E, Campanella S, Taylor SL, Roberts SA.** 2007. *Haemophilus ducreyi* causing chronic skin ulceration in children visiting Samoa. Clin. Infect. Dis. **44:**e85–e87. http://dx.doi.org/10.1086/515404.
4. **McBride WJ, Hannah RC, Le Cornec GM, Bletchly C.** 2008. Cutaneous chancroid in a visitor from Vanuatu. Australas. J. Dermatol. **49:**98–99. http://dx.doi.org/10.1111/j.1440-0960.2008.00439.x.
5. **Peel TN, Bhatti D, De Boer JC, Stratov I, Spelman DW.** 2010. Chronic cutaneous ulcers secondary to *Haemophilus ducreyi* infection. Med. J. Aust. **192:**348–350.
6. **Mitjà O, Lukehart SA, Pokowas G, Moses P, Kapa A, Godornes C,** **Robson J, Cherian S, Houinei W, Kazadi W, Siba P, de Lazzari E, Bassat Q.** 2014. *Haemophilus ducreyi* as a cause of skin ulcers in children from a yaws-endemic area of Papua New Guinea: a prospective cohort study. Lancet Global Health **2:**e235–e241. http://dx.doi.org/10.1016/S2214-109X(14)70019-1.
7. **Janowicz DM, Ofner S, Katz BP, Spinola SM.** 2009. Experimental infection of human volunteers with *Haemophilus ducreyi*: fifteen years of clinical data and experience. J. Infect. Dis. **199:**1671–1679. http://dx.doi.org/10.1086/598966.
8. **Bauer ME, Goheen MP, Townsend CA, Spinola SM.** 2001. *Haemophilus ducreyi* associates with phagocytes, collagen, and fibrin and remains extracellular throughout infection of human volunteers. Infect. Immun. **69:**2549–2557. http://dx.doi.org/10.1128/IAI.69.4.2549-2557.2001.
9. **Bauer ME, Townsend CA, Ronald AR, Spinola SM.** 2006. Localization of *Haemophilus ducreyi* in naturally acquired chancroidal ulcers. Microbe Infect. **8:**2465–2468. http://dx.doi.org/10.1016/j.micinf.2006.06.001.
10. **Spinola SM, Fortney KR, Baker B, Janowicz DM, Zwickl B, Katz BP, Blick RJ, Munson RS, Jr.** 2010. Activation of the CpxRA system by deletion of *cpxA* impairs the ability of *Haemophilus ducreyi* to infect humans. Infect. Immun. **78:**3898–3904. http://dx.doi.org/10.1128/IAI.00432-10.
11. **Gangaiah D, Zhang X, Fortney KR, Baker B, Liu Y, Munson RS, Jr, Spinola SM.** 2013. Activation of CpxRA in *Haemophilus ducreyi* primarily inhibits the expression of its targets, including major virulence determinants. J. Bacteriol. **195:**3486–3502. http://dx.doi.org/10.1128/JB.00372-13.
12. **Labandeira-Rey M, Brautigam CA, Hansen EJ.** 2010. Characterization of the CpxRA regulon in *Haemophilus ducreyi*. Infect. Immun. **78:**4779–4791. http://dx.doi.org/10.1128/IAI.00678-10.
13. **Labandeira-Rey M, Dodd D, Fortney KR, Zwickl B, Katz BP, Janowicz DM, Spinola SM, Hansen EJ.** 2011. A *Haemophilus ducreyi cpxR* deletion mutant is virulent in human volunteers. J. Infect. Dis. **203:**1859–1865. http://dx.doi.org/10.1093/infdis/jir190.
14. **Ades SE.** 2008. Regulation by destruction: design of the sigmaE envelope stress response. Curr. Opin. Microbiol. **11:**535–540. http://dx.doi.org/10.1016/j.mib.2008.10.004.
15. **Ruiz N, Silhavy TJ.** 2005. Sensing external stress: watchdogs of the *Escherichia coli* cell envelope. Curr. Opin. Microbiol. **8:**122–126. http://dx.doi.org/10.1016/j.mib.2005.02.013.
16. **Alba BM, Gross CA.** 2004. Regulation of the *Escherichia coli* sigmaE-dependent envelope stress response. Mol. Microbiol. **52:**613–619. http://dx.doi.org/10.1111/j.1365-2958.2003.03982.x.
17. **Raivio TL, Silhavy TJ.** 2001. Periplasmic stress and ECF sigma factors. Annu. Rev. Microbiol. **55:**591–624. http://dx.doi.org/10.1146/annurev.micro.55.1.591.
18. **De Las Penas A, Connolly L, Gross CA.** 1997. The sigmaE-mediated response to extracytoplasmic stress in *Escherichia coli* is transduced by RseA and RseB, two negative regulators of sigmaE. Mol. Microbiol. **24:**373–385. http://dx.doi.org/10.1046/j.1365-2958.1997.3611718.x.
19. **Missiakas D, Mayer MP, Lemaire M, Georgopoulos C, Raina S.** 1997. Modulation of the *Escherichia coli* sigmaE (RpoE) heat-shock transcription-factor activity by the RseA, RseB and RseC proteins. Mol. Microbiol. **24:**355–371. http://dx.doi.org/10.1046/j.1365-2958.1997.3601713.x.
20. **Rowley G, Spector M, Kormanec J, Roberts M.** 2006. Pushing the envelope: extracytoplasmic stress responses in bacterial pathogens. Nat. Rev. Microbiol. **4:**383–394. http://dx.doi.org/10.1038/nrmicro1394.
21. **Chaba R, Alba BM, Guo MS, Sohn J, Ahuja N, Sauer RT, Gross CA.** 2011. Signal integration by DegS and RseB governs the sigmaE-mediated envelope stress response in *Escherichia coli*. Proc. Natl. Acad. Sci., U. S. A. **108:**2106–2111. http://dx.doi.org/10.1073/pnas.1019277108.
22. **Lima S, Guo MS, Chaba R, Gross CA, Sauer RT.** 2013. Dual molecular signals mediate the bacterial response to outer-membrane stress. Science **340:**837–841. http://dx.doi.org/10.1126/science.1235358.
23. **Rhodius VA, Suh WC, Nonaka G, West J, Gross CA.** 2006. Conserved and variable functions of the sigmaE stress response in related genomes. PLoS Biol. **4:**e2. http://dx.doi.org/10.1371/journal.pbio.0040002.
24. **Bury-Mone S, Nomane Y, Reymond N, Barbet R, Jacquet E, Imbeaud S, Jacq A, Bouloc P.** 2009. Global analysis of extracytoplasmic stress signaling in *Escherichia coli*. PLoS Genet. **5:**e1000651. http://dx.doi.org/10.1371/journal.pgen.1000651.
25. **De Las Penas A, Connolly L, Gross CA.** 1997. SigmaE is an essential sigma factor in *Escherichia coli*. J. Bacteriol. **179:**6862–6864.
26. **Hayden JD, Ades SE.** 2008. The extracytoplasmic stress factor, sigmaE, is

required to maintain cell envelope integrity in *Escherichia coli*. PLoS One **3**:e1573. http://dx.doi.org/10.1371/journal.pone.0001573.

27. **Harrison A, Santana EA, Szelestey BR, Newsom DE, White P, Mason KM.** 2013. Ferric uptake regulator and its role in the pathogenesis of nontypeable *Haemophilus influenzae*. Infect. Immun. **81**:1221–1233. http://dx.doi.org/10.1128/IAI.01227-12.

28. **Whitby PW, Morton DJ, Stull TL.** 1998. Construction of antibiotic resistance cassettes with multiple paired restriction sites for insertional mutagenesis of *Haemophilus influenzae*. FEMS Microbiol. Lett. **158**:57–60. http://dx.doi.org/10.1111/j.1574-6968.1998.tb12800.x.

29. **Lee EC, Yu D, Martinez de Velasco J, Tessarollo L, Swing DA, Court DL, Jenkins NA, Copeland NG.** 2001. A highly efficient *Escherichia coli*-based chromosome engineering system adapted for recombinogenic targeting and subcloning of BAC DNA. Genomics **73**:56–65. http://dx.doi.org/10.1006/geno.2000.6451.

30. **Huang da W, Sherman BT, Lempicki RA.** 2009. Systematic and integrative analysis of large gene lists using DAVID bioinformatics resources. Nat. Protoc. **4**:44–57. http://dx.doi.org/10.1038/nprot.2008.211.

31. **Bailey TL, Elkan C.** 1994. Fitting a mixture model by expectation maximization to discover motifs in biopolymers. Proc. Int. Conf. Intell. Syst. Mol. Biol. **2**:28–36.

32. **Mao F, Dam P, Chou J, Olman V, Xu Y.** 2009. DOOR: a database for prokaryotic operons. Nucleic Acids Res. **37**:D459–D463. http://dx.doi.org/10.1093/nar/gkn757.

33. **Liu Y, Taylor MW, Edenberg HJ.** 2006. Model-based identification of cis-acting elements from microarray data. Genomics **88**:452–461. http://dx.doi.org/10.1016/j.ygeno.2006.04.006.

34. **Cormack BP, Valdivia RH, Falkow S.** 1996. FACS-optimized mutants of the green fluorescent protein (GFP). Gene **173**:33–38. http://dx.doi.org/10.1016/0378-1119(95)00685-0.

35. **Schneider CA, Rasband WS, Eliceiri KW.** 2012. NIH Image to ImageJ: 25 years of image analysis. Nat. Methods **9**:671–675. http://dx.doi.org/10.1038/nmeth.2089.

36. **Gangaiah D, Labandeira-Rey M, Zhang X, Fortney KR, Ellinger S, Zwickl B, Baker B, Liu Y, Janowicz DM, Katz BP, Brautigam CA, Munson RS, Jr, Hansen EJ, Spinola SM.** 2014. *Haemophilus ducreyi* Hfq contributes to virulence gene regulation as cells enter stationary phase. mBio **5**(1):e01028-13. http://dx.doi.org/10.1128/mBio.01081-13.

37. **Battesti A, Majdalani N, Gottesman S.** 2011. The RpoS-mediated general stress response in *Escherichia coli*. Annu. Rev. Microbiol. **65**:189–213. http://dx.doi.org/10.1146/annurev-micro-090110-102946.

38. **Price NL, Raivio TL.** 2009. Characterization of the Cpx regulon in *Escherichia coli* strain MC4100. J. Bacteriol. **191**:1798–1815. http://dx.doi.org/10.1128/JB.00798-08.

39. **Connolly L, De Las Penas A, Alba BM, Gross CA.** 1997. The response to extracytoplasmic stress in *Escherichia coli* is controlled by partially overlapping pathways. Genes Dev. **11**:2012–2021. http://dx.doi.org/10.1101/gad.11.15.2012.

40. **Raivio TL, Leblanc SK, Price NL.** 2013. The *Escherichia coli* Cpx envelope stress response regulates genes of diverse function that impact antibiotic resistance and membrane integrity. J. Bacteriol. **195**:2755–2767. http://dx.doi.org/10.1128/JB.00105-13.

41. **Al-Tawfiq JA, Thornton AC, Katz BP, Fortney KR, Todd KD, Hood AF, Spinola SM.** 1998. Standardization of the experimental model of *Haemophilus ducreyi* infection in human subjects. J. Infect. Dis. **178**:1684–1687. http://dx.doi.org/10.1086/314483.

42. **Dixon LG, Albritton WL, Willson PJ.** 1994. An analysis of the complete nucleotide sequence of the *Haemophilus ducreyi* broad-host-range plasmid pLS88. Plasmid **32**:228–232. http://dx.doi.org/10.1006/plas.1994.1060.